Chevallier, Julien

Article

COVID-19 pandemic and financial contagion

Journal of Risk and Financial Management

Provided in Cooperation with:
MDPI – Multidisciplinary Digital Publishing Institute, Basel

Suggested Citation: Chevallier, Julien (2020) : COVID-19 pandemic and financial contagion, Journal of Risk and Financial Management, ISSN 1911-8074, MDPI, Basel, Vol. 13, Iss. 12, pp. 1-25,
https://doi.org/10.3390/jrfm13120309

This Version is available at:
https://hdl.handle.net/10419/239395

Journal of
Risk and Financial Management

MDPI

Article

COVID-19 Pandemic and Financial Contagion

Julien Chevallier [1,2]

[1] Department of Economics & Management, IPAG Business School (IPAG Lab), 184 bd Saint-Germain, 75006 Paris, France; julien.chevallier@ipag.fr
[2] Economics Department, Université Paris 8 (LED), 2 rue de la Liberté, CEDEX 93526 Saint-Denis, France

Received: 15 October 2020; Accepted: 1 December 2020; Published: 3 December 2020

Abstract: The original contribution of this paper is to empirically document the contagion of the COVID-19 on financial markets. We merge databases from Johns Hopkins Coronavirus Center, Oxford-Man Institute Realized Library, NYU Volatility Lab, an d St-Louis Federal Reserve Board. We deploy three types of models throughout our experiments: (i) the Susceptible-Infective-Removed (SIR) that predicts the infections' peak on 2020-03-27; (ii) volatility (GARCH), correlation (DCC), and risk-management (Value-at-Risk (VaR)) models that relate how bears painted Wall Street red; and, (iii) data-science trees algorithms with forward prunning, mosaic plots, and Pythagorean forests that crunch the data on confirmed, deaths, and recovered COVID-19 cases and then tie them to high-frequency data for 31 stock markets.

Keywords: COVID-19; financial contagion; Johns Hopkins repository; Susceptible-Infective-Removed model; tree algorithm; data science

1. Introduction

The COVID-19 pandemic hit the world economy, without anyone knowing, at light-speed, leading to partial unemployment and factories' shutdown around the globe, leaving doctors, policymakers, businessmen, operational managers, data scientists, and citizens alike in disarray. The origin of the virus itself is not known with certainty, although most theories attach it to zoonotic transfer to the human species (Andersen et al. 2020).

As such, the COVID-19 virus outbreak represents a pandora's box. The original 45-day lock-down in most industrialized countries dated mid-March 2020 took everybody off-guard. This paper aims to address many viewpoints (e.g., business cycle analysis, operational research impediments, open-data science) during this traumatizing event.

With the quarantine in action in most industrialized countries from mid-March until the end-of-year 2020, many economist observers predict a deep recession for 2021–22. Stock markets plunged in March–April 2020, due to the shocking news of the virus spreading around the world.

Literature on the financial impacts of the COVID-19 is burgeoning. Akhtaruzzaman et al. (2020) examine how financial contagion occurs through financial and nonfinancial firms between China and G7 countries during the COVID–19 period. Ashraf (2020) finds that stock market returns declined as the number of COVID-19 confirmed cases increased. Among the main driving forces, government restrictions on commercial activity and voluntary social distancing are the main reasons behind the U.S. stock market plunge (Baker et al. 2020). On the Chinese stock market, Al-Awadhi et al. (2020) confirm that the daily growth in the total confirmed cases and total cases of death caused by COVID-19 both have significant negative effects on stock returns across all companies. Papadamou et al. (2020) suggest that Google-based anxiety regarding COVID-19 contagion effects leads to elevated risk-aversion in stock markets. Sharif et al. (2020b) analyze the connectedness between the recent spread of COVID-19, oil price volatility shock, the stock market, geopolitical risk, and economic policy uncertainty in

the US within a time-frequency framework. Regarding the stringency of policy responses to the novel coronavirus pandemic worldwide, Zaremba et al. (2020) demonstrate that non-pharmaceutical interventions significantly increase equity market volatility. Ji et al. (2020) evaluate the safe-haven role of assets in the current COVID-19 pandemic (gold and soybean futures). Shifting away from traditional asset markets, Conlon and McGee (2020) show that a small allocation to Bitcoin substantially increases portfolio downside risk: cryptocurrencies move in lockstep with the S&P 500 as the crisis develops. In the same vein, Cheema et al. (2020) identify that, during COVID, investors might have lost trust in gold. The US dollar has acted as a safe haven only for China and India during COVID. However, tether can be seen as a strong safe-haven.

In this paper, we seek to analyze how the sanitary crisis impacted economic activity based on various methodological frameworks: a Susceptible-Infective-Removed model (epidemiology); GARCH, Dynamic Conditional Correlation, and Value-at-Risk (finance); Decision Tree Algorithm with Forward Pruning, Mosaic Plot, and Pythagorean Forest (data science).

The study unfolds by (i) reporting statistics and evidence on the evolution of the pandemic, (ii) analyzing the impact of the crisis on financial markets, and (iii) presenting a case study regarding how data science can be applied to link financial data to Covid-data.

From a financial contagion[1] viewpoint, we uncover a wealth of insights that are related to the COVID-19 virus outbreak. According to the infectious model, the most noticeable result was the world's infection "peak" detected on 3 March. According to the decision tree, the virus contamination has been irrigating worldwide stock markets since mid-March 2020, stemming from Western Europe's France CAC 40 (with President Macron establishing 45-day lock-down on 16 March).

The article's motivation is to elaborate, against the pandemic background, a data-driven academic assessment of the financial meltdown at stake. The article's primary purpose is to confront many viewpoints on the COVID-19 epidemic: medical professionals, financial analysts, and data scientists. The goals are to retrieve scientific data in order to make statements regarding financial market contagion. The novelty is in conducting empirical experiments from the technical standpoints of data-science and operations research. The contribution is to be found in the financial literature by providing several stylized facts on how financial markets react and can be expected to recover from the COVID-19 pandemic.

In terms of methodology, we show, using operational research models, that asset markets were linked to the spread of the COVID-19 stocks panic across the globe. The central result is that COVID-19 triggered an unexpected panic on stock markets, which all went into losses territory. Asset managers do not have sufficient "safe-assets" to hedge against this market panic. Therefore, the stock markets' critical message is to wait for the COVID-19 vaccine to loom on the horizon: as more patients recover from the disease, a new era of market gains will begin. The empirical observation that asset markets could be re-born as patients heal and the hopes of a vaccine against COVID-19 become realistic is genuinely novel.

---

[1] To elaborate on the notion of "contagion" in financial econometrics, usually, the definition by Forbes and Rigobon (2002) is retained as a significant increase in cross-market linkages after a shock to one country (or group of countries). According to this definition, if two markets show a high degree of co-movement during periods of stability, even if the markets continue to be positively correlated after a shock to one market, then this may not constitute contagion. According to Forbes and Rigobon (2002)'s definition, it is only contagion if cross-market co-movement significantly increases after the shock. If the co-movement does not increase significantly, then any continued high level of market correlation suggests strong linkages between the two economies that exist in all states of the world. The term interdependence is used to refer to this situation. In our setting, we merely employ financial econometrics techniques (e.g., GARCH, Dynamic Conditional Correlation (DCC), Value-at-Risk (VaR)) in order to describe the state of disarray on financial markets given the whole pandemic situation. We are not interested in measuring excess co-movements. The paper's original contribution lies in the data-scientist approach, instead mobilizing operational research techniques.

To retrieve data, we connected remotely to the servers of the John Hopkins Coronavirus Resource Center[2], the Oxford-Man Institute Realized Library[3], the Volatility Lab at New York University[4], and the St-Louis Federal Reserve Board[5,6]. The time frame for the window of observations differs whether we access only recent (newest) data, such as COVID-19 cases, or whether we download the full history of data of prices for financial markets in order to document the current historical peaks.[7]

The remainder of the article is structured, as follows. Section 2 details the latest medical evidence on the virus. Section 3 depicts the disarray of investors. Section 4 connects the epidemiological cases on COVID-19 to the contagion that was witnessed on financial markets from a data-science perspective. Section 5 concludes.

2. Epidemiological Evidence on the Widespread COVID-19

2.1. Inspecting the Tank of Johns Hopkins Coronavirus Resource Center

At the time of writing the article (2020-05-06), the Johns Hopkins Center on Coronavirus totaled 3,662,691 confirmed cases, 257,239 deaths, and 1,198,832 recovered cases worldwide. Figure 1 presents recent trends.

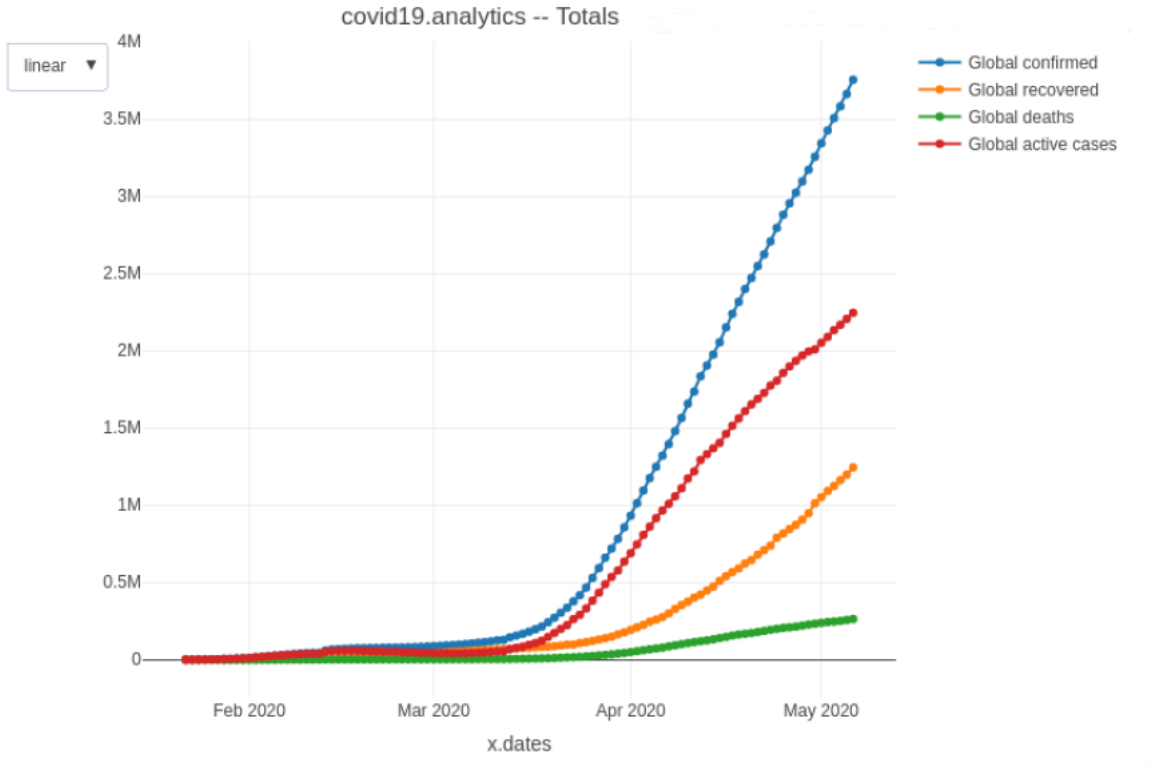

Figure 1. Aggregated COVID-19 accessed from JHU/CCSE repository on 2020-05-05.

---

2 https://Coronavirus.jhu.edu/.
3 https://realized.oxford-man.ox.ac.uk/.
4 https://vlab.stern.nyu.edu/.
5 https://fred.stlouisfed.org/.
6 Regarding the computational setting, the statistics are running via GNU software on an IA-ready UNIX workstation equipped with an i7-9700K @ 3.60 GHz × 8 CPU, 2 TB NVMe SSD, and 32 GiB RAM.
7 The data retrieved from the John Hopkins Coronavirus Resource Center is in daily frequency (COVID-19 reported cases). Data from the Volatility Lab NYU are presented in daily frequency (for GARCH and DCC estimates) and from the St-Louis Federal Reserve Board (VIX and Stress index). The data are only in high-frequency in the case of financial markets data from Oxford University servers.

Figure 1 displays the exponentially increasing number of global COVID-19 cases that are characteristic of the pandemic (at the time of extraction from the Johns Hopkins repository). In May 2020, this highly contagious virus had spread over the five continents of the Earth and infected more than 4.2 million people in more than 187 countries (out of 198 in total). When writing the paper, the United States had the highest number of infected individuals, followed by China, Italy, and Iran.

In the Appendix A, we provide additional insights on this exhaustive database, namely aggregated data that are ordered by confirmed cases, deaths, recovered cases, and active cases in Tables A1–A4. Besides, Tables A5–A7 present detailed statistics on the top-10 contributors (by country) in terms of confirmed cases, deaths, and recovered cases.

2.2. A Susceptible-Infective-Removed (SIR) Model for the World

In Figure 2, we provide the Susceptible-Infective-Removed (SIR) model by Bailey (1975) for the World.

This model supposes that we have a closed, homogeneously mixing population divided into $X(t)$ susceptible, $Y(t)$ infective, and $Z(t)$ removed individuals at time t. The initial conditions are set to $X(0) = N, Y(0) = a, Z(0) = 0$ for some N, a. Because the population is closed, we have $X(t) + Y(t) + Z(t) = N + a$ for all $t \geq 0$, so that the epidemic is completely described by the process $\{(X(t), Y(t)), t \geq 0\}$. The epidemic is assumed to a continuous-time Markov process on the state space:

$$D_{N,a} = \{(x, y) \in \mathbb{Z}^2 : 0 \leq x \leq N, y \geq 0, x + y \leq N + a\} \tag{1}$$

Transition probabilities are given by:

$$Pr((X(t + \delta t)), Y(t + \delta t)) = (x - 1, y + 1) | (X(t), Y(t)) = (x, y) = \beta x y \delta t + \xi(\delta t), \tag{2}$$

$$Pr((X(t + \delta t)), Y(t + \delta t)) = (x, y - 1) | (X(t), Y(t)) = (x, y) = \gamma y \delta t + \xi(\delta t) \tag{3}$$

All other transitions have probability $\xi(\delta t)$, and the parameters $\beta > 0$, $\gamma > 0$, being known as the infection rate and removal rate, respectively. The process terminates when the number of infectives becomes zero, which will almost surely happen within finite time. Further mathematical derivation is covered, for instance, in Clancy (2014). The SIR model has been applied, among others, by Shamsi et al. (2018) for post-disaster vaccine provision. Table 1 presents the estimated parameters.

Table 1. Parameter estimates for the Susceptible-Infective-Removed (SIR) Model.

Parameters used to create the SIR model	
Region:	ALL
Time interval to consider: $t_0 = 1$; $t_1 = 15$; $t_{final} = 90$	
t_0: 2020-01-23	t_1: 2020-02-06
Number of days considered for the initial guess: 15	
Fatality rate: 0.02	
Population of the region: 7 800 000 000	
Convergence: Relative Reduction of F $\leftarrow$ FACTR $\times$ EPSMCH	
beta	gamma
0.6442002	0.3557998
R_0= 1.81056940871835	
Max of infected: 931947691.37 (11.95%)	
Max nbr of casualties, assuming 2.00% fatality rate: 18638953.83	
Max reached at day: 57 $\rightarrow$ 2020-03-20	

According to the estimates, the "peak" of infections stemming from COVID-19 was reached on 3 March 2020, which justifies the 45-day lock-down that was implemented in most industrialized countries at the time. Figure 2 reflects the likely trends for the evolution of the epidemic.

The lock-down's intended effect is to witness a decrease in the contamination level from the COVID-19 and the number of infected.

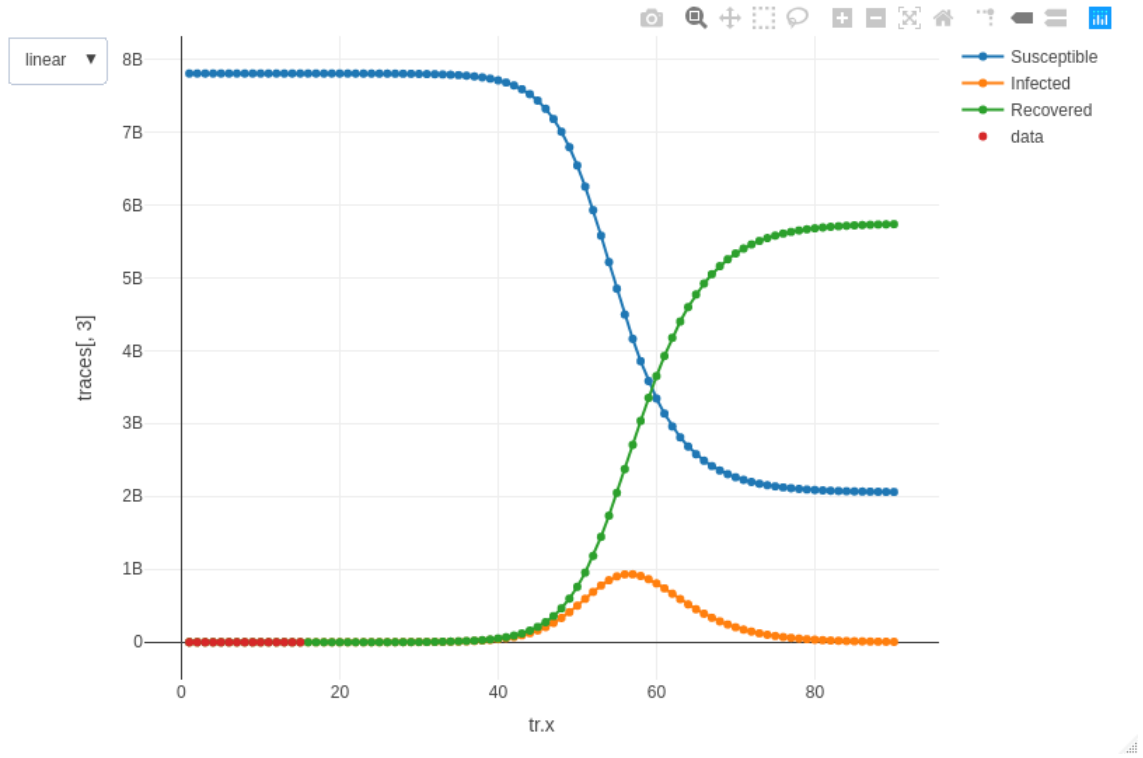

Figure 2. SIR Model for the World on all data available from JHU/CCSE repository on 2020-05-05.

Having covered what medical science can tell us (at the time of writing) regarding the COVID-19 pandemic, we wish to envision how it impacted the world economy in the next section.

3. Asset Markets: The Nightmare Scenario

At the start of the global Covid-2019 pandemic in 2020, the financial markets entered a period of enormous financial stress. Corbet et al. (2020) indicate that the volatility relationship between the main Chinese stock markets and Bitcoin has evolved considerably during this tension period. Gunay (2020b) finds that the COVID-19 pandemic caused a different and more severe version of the contagion phenomenon in six different stock markets, such as the United States, Italy, Spain, China, the United Kingdom, and Turkey. Sharif et al. (2020a) assert that COVID-19 constitutes a significant threat for the U.S. stock market and carries geopolitical risk. The COVID-19 risk is perceived differently over the short- and the long-run, and it may be first viewed as an economic crisis.

The purpose of this section is to establish a quantitative assessment of the economic and financial consequences of the COVID-19 spreading worldwide, with a statistical assessment of (i) volatility, (ii) asset allocation, and (iii) risk management.

3.1. A Volatility Perspective

Things went south very quickly on stock markets. Global stock markets erased approximately six-trillion U.S. dollars in wealth in one week from 24 to 28 February due to fear and uncertainty and the rational assessment of investors that firms' profits are likely to be lower due to the impact of COVID-19. On 16 March 2020, the Dow Jones plummeted nearly 3000 points. Bonds, oil, and gold dropped in sync. During the week of 24 March 2020, the S&P 500 experienced its worst week since the 2008 sub-prime crisis. As can be expected, fear indexes exploded during that period, such as the

VIX (which is computed from options on the S&P 500), or the Financial stress index computed by the St-Louis Federal Reserve board, which peaked at a year-on-year high (see Figure 3).

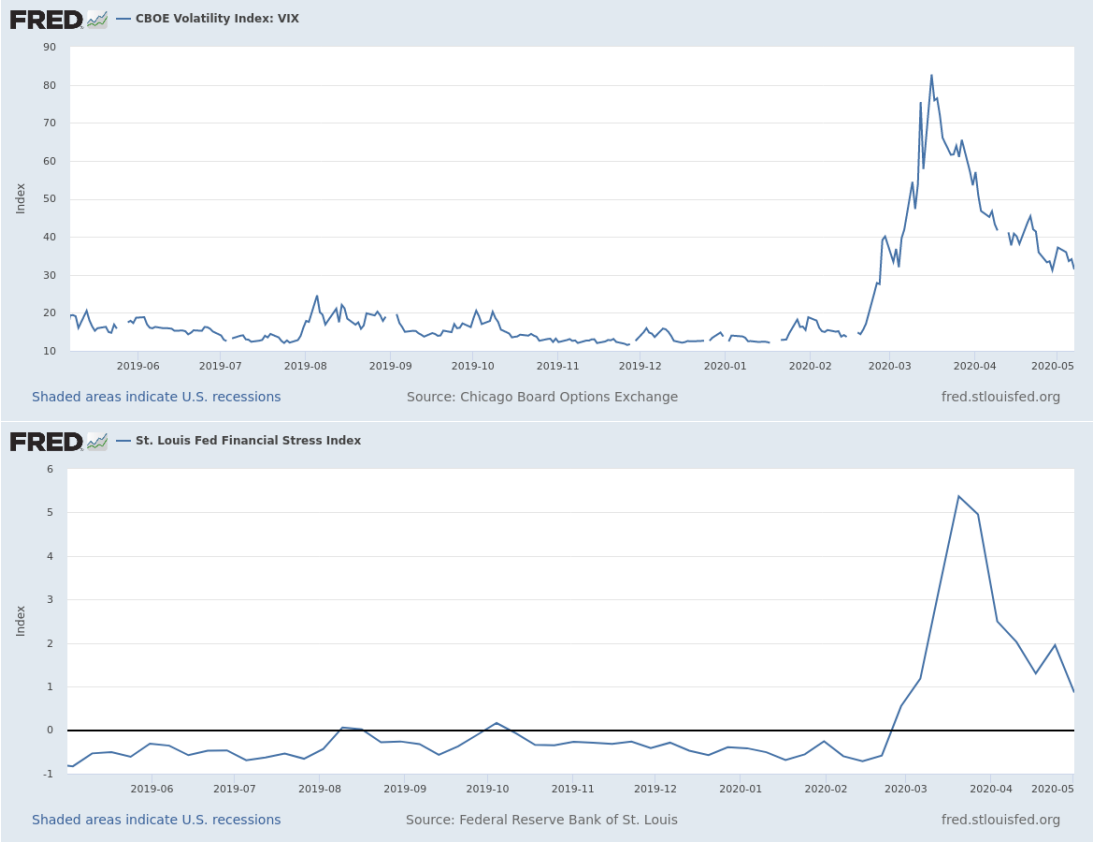

Figure 3. CBOE Volatility Index VIX (**top**) and St. Louis Fed Financial Stress Index (**bottom**) from 2019-05-07 to 2020-05-07. Note: The graph is produced by Board of Governors of the Federal Reserve System (US) and the St-Louis Federal Reserve (FRED). VIX: Index, Not Seasonally Adjusted. Frequency: Daily, Close. Financial Stress: Index, Not Seasonally Adjusted. Frequency: Weekly, Ending Friday.

In terms of macroeconomic fundamentals, a severe economic downturn is to be expected. Its depth can only be foreshadowed based on a preliminary inspection of industrial production data, which dropped considerablt with the 45-day lock-down that was implemented in most industrialized countries (see Figure 4). OECD countries, developing countries, and least-developed countries will experience differentiated impacts. For instance, some countries will be more severely impacted by others' closing of trading routes, depending on the price of commodities to be exported to international trade markets.

Zhang et al. (2020) have already covered some ground on the COVID-19 sanitary crisis's financial aspects. By utilizing graph theory and the minimum spanning tree technique, they map the general patterns of country-specific risks and systemic risks in the global financial markets. Regional market integration/collaboration is likely to appear in the face of this major crisis.

Bae et al. (2003) helps us to define contagion on financial markets by distinguishing between the terms "Epidemics" (when the virus effects are spread within geographical regions) and "Pandemics" (when its effects are prevalent across regions). The latter category is characterized by threshold events of "infection", similar to what we have witnessed in mid-March 2020. Real and financial consequences of such outbursts are to be expected.

The volatility during this window of time goes through the roof (e.g., documented as high as 49.93% in April 2020 based on a GARCH(1,1) analysis for the S&P 500 index), as presented in Figure 5. Besides, in Table 2, we verify that all of the parameters are positive and significant.

According to Bollerslev (1986), the latent volatility process can, indeed, be extracted by modeling the conditional variance in a Generalized Autoregressive Conditional Heteroskedasticity model: $\sigma_t^2 = \omega + \alpha\epsilon_{t-1}^2 + \beta\sigma_{t-1}^2$. σ_t^2 is the conditional volatility and ϵ_{t-1}^2 the squared unexpected returns from previous period. Restrictions apply: ω >0 and $\alpha + \beta < 1$. Table 2 contains parameter estimates for daily volatility. GARCH is now on the dashboard of all asset managers across the industry. The main parameters of interest are finding positive values (because we are dealing with variances) and statistical significance. The sum of alpha and beta shall be below unity (otherwise, it indicates the need to estimate GARCH-variants).

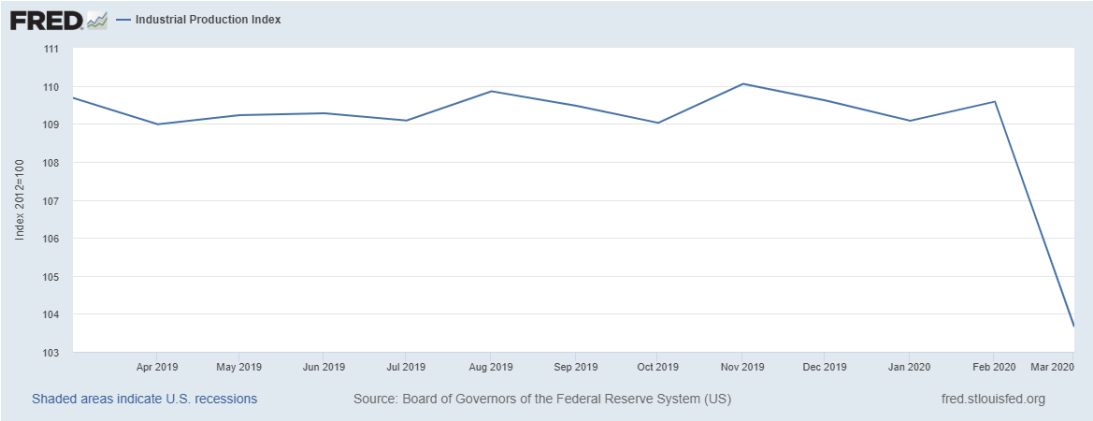

Figure 4. US Industrial Production Index from 2019-03-01 to 2020-03-01. Note: the graph is produced by Board of Governors of the Federal Reserve System (US) and the St-Louis Federal Reserve (FRED). Index 2012 = 100. Seasonally Adjusted. Frequency: Monthly.

Table 2. GARCH(1,1) Parameter estimates and Volatility analysis for the S&P 500 index.

Parameter Estimates					
	param	t-stat			
ω	0.0154	18.40			
α	0.0934	38.62			
β	0.8934	383.26			
Volatility Summary					
Closing Price:	$2868.44	Return:	0.90%	1 Week Pred:	33.14%
Average Week Vol:	36.17%	Average Month Vol:	49.93%	1 Month Pred:	31.92%
Min Vol:	6.90%	Max Vol:	89.88%	6 Month Pred:	26.41%
Average Vol:	17.70%	Vol of Vol:	23.27%	1 Year Pred:	23.09%

Note: The Estimation period is 2 January 1990 to 1 May 2020.

3.2. An Asset Manager's Perspective

For skilled traders in the derivatives markets, this pandemic might provide them opportunities to enhance their Profit & Loss statement. However, for most pension funds, mutual fund investors, and risk managers, there is "no place to hide" (Buraschi et al. 2014) in the cross-section of returns when dealing with conventional asset markets (e.g., stocks, bonds, foreign exchange, commodities) or even with gold Exchange-Traded funds.

Figure 6 documents an unprecedentedly high level of correlation among international equities, peaking at 88.93% in April 2020, thereby strengthening the contagion scenario. Correlation analysis runs by construction from (−1) in blue to (+1) in red. There are opportunities for uncorrelated investment for the asset manager whenever the blue color is present (which is what he is looking for according to Markowitz portfolio theory). Only correlated market movements appear in the current context, which means that the asset manager has no solution to transfer his funds.

According to Engle and Sheppard (2001), correlations among assets can be captured through a Dynamic Conditional Correlation model. A general dynamic correlation structure follows:

$$\left\{ Q_t = S \circ (ii' - A - B) + A \circ Z_{t-1} Z'_{t-1} + B \circ Q_{t-1}; R_t = \text{diag}\{Q_t\}^{-\frac{1}{2}} Q_t \text{diag}\{Q_t^{-\frac{1}{2}}\} \right\} \quad (4)$$

where S is the unconditional variance of the standardized residuals. i is a vector of ones. $\circ$ is the Hadamard product of two identically sized matrices. If A, B, and $ii' - A - B$ are positive semi-definite, then Q will be positive semi-definite. R_t is the time-varying correlation matrix.

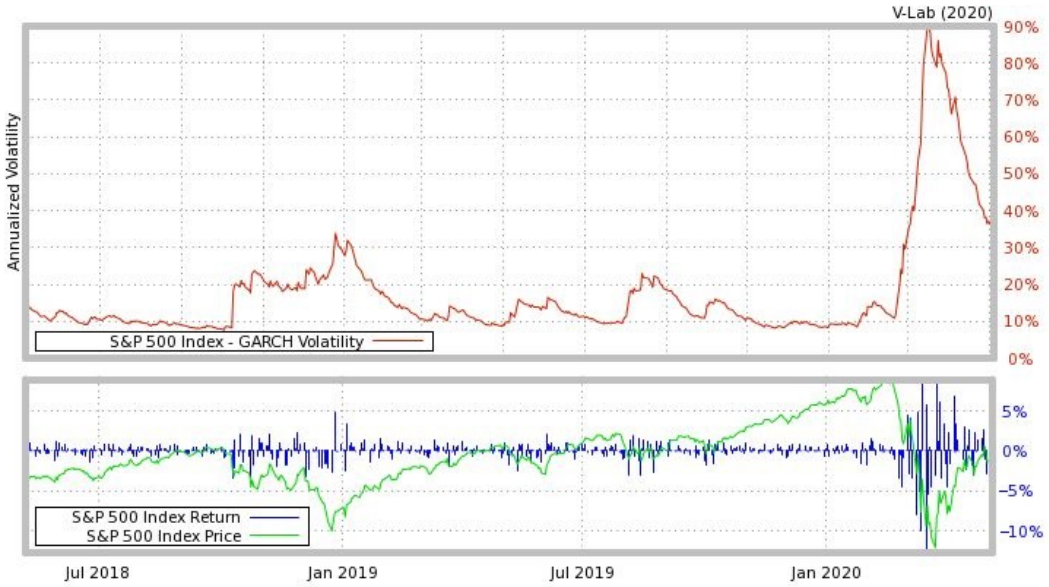

Figure 5. Volatility Analysis for the S&P 500 index as extracted from GARCH(1,1). Note: The graph is produced by NYU Volatility Lab. The Estimation period is 2 January 1990 to 1 May 2020.

In Table 3, we verify that the DCC(1,1) correlation parameters are all positive and statistically significant. Table 3 presents correlation estimates (not volatility). We are interested in recovering statistically significant estimates with a sum of alpha and beta below one (otherwise, misspecification tests are required). The DCC matrix gives the level of correlation. In our case, it displays an all-time high correlation level of 88% across asset markets (henceforth, our research question of contagion due to the COVID-19 pandemic).

In the Appendix A, the interested reader may observe that the picture is the same across other asset markets (e.g., historical peak in correlations recorded for bonds and commodities in Figures A1 and A2). Foreign exchange markets are "frozen" due to the halt of international trade routes (i.e., the correlation is decreasing in Figure A3).

Table 3. DCC(1,1) Parameter estimates and Correlation analysis.

Parameter estimates		
	param	t-stat
α	0.0096	29.69
β	0.9832	1456.52
Correlation Summary Table		
Lower Corr:	0.4739	
Upper Corr:	0.8893	
1st Factor:	0.7562	
2nd Factor:	0.0446	

Note: The Estimation period is 15 April 2003 to 1 May 2020.

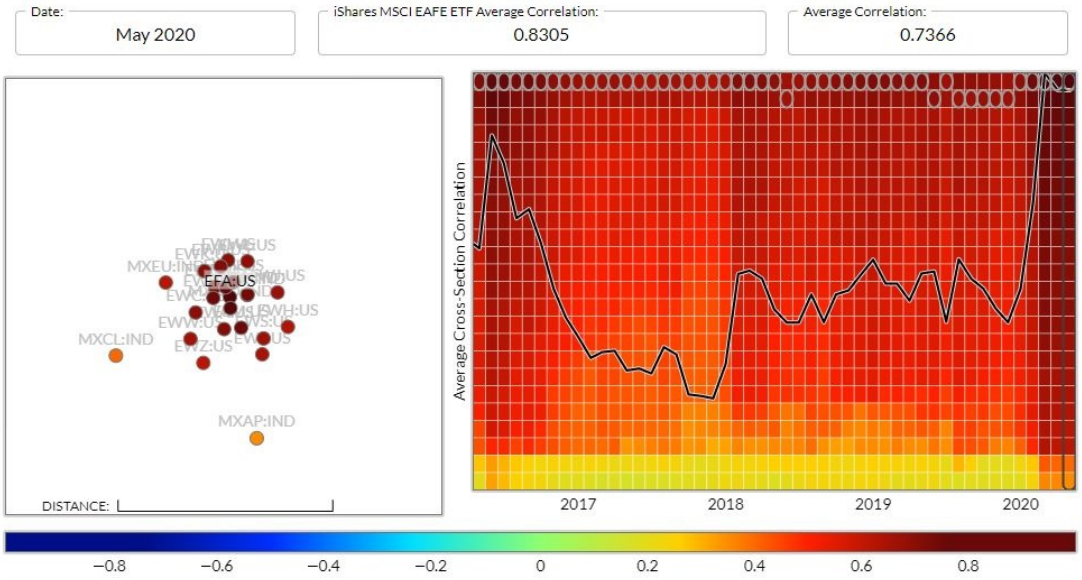

Figure 6. Correlation Analysis for International Equities as extracted from DCC(1,1). Note: The graph is produced by NYU Volatility Lab. The Estimation period is 15 April 2003 to 1 May 2020. The International Equities dataset contains the following series: iShares MSCI Australia ETF (EWA) iShares MSCI Belgium Capped ETF (EWK) iShares MSCI Brazil Capped ETF (EWZ) iShares MSCI Canada ETF (EWC) iShares MSCI EAFE ETF (EFA) iShares MSCI Emerging Markets ETF (EEM) iShares MSCI Germany ETF (EWG) iShares MSCI Hong Kong ETF (EWH) iShares MSCI Italy Capped ETF (EWI) iShares MSCI Japan ETF (EWJ) iShares MSCI Mexico Capped ETF (EWW) iShares MSCI Netherlands ETF (EWN) iShares MSCI Singapore Capped ETF (EWS) iShares MSCI Spain Capped ETF (EWP) iShares MSCI Sweden Capped ETF (EWD) iShares MSCI Switzerland Capped ETF (EWL) iShares MSCI Taiwan Capped ETF (EWT) iShares MSCI United Kingdom ETF (EWU) MSCI Asia Pacific (MXAP) MSCI Chile (MXCL) MSCI Europe (MXEU) MSCI USA (MXUS) MSCI World (MXWD) S&P 500 Index (SPX).

For digital assets, such as Bitcoin, the deep price plunge that followed the aftermath of the S&P 500 market crash (as illustrated in Figure 7) tells us that they cannot be deemed as a store for value either. The correlation coefficient between SP500 and CBBTCUSD is computed as 0.83 since the beginning of the year 2020[8]. Hence, the popular wisdom that "cash is king" seems to currently prevail.

3.3. A Risk-Manager's Perspective

The Value-at-Risk (VaR), a that was concept popularized by Jorion (2000)[9], has also known a "black-swan" (Taleb 2007) event during March–April 2020, with virtually all holdings from liquidity risks passing below the 5% threshold usually retained by risk managers. The realization of such an important risk measure from a risk management perspective is visible in Figure 8.

This all circles back to the notion of systemic risk that is caused by the pandemic. Systemic risk refers to the disruption of an economy's financial system's proper functioning emanating from shocks from within or outside the financial system (Martínez-Jaramillo et al. 2010). While numerous policymakers are exploring the pandemic's economic impact, lessons that are learned from the global financial crisis demand the evaluation of financial stability concerning the effective management of the

---

[8] Spearman rank correlation is equal to 0.84, and Kendall's tau is equal to 0.66.

[9] The single-period (n = 1) 1$ VaR on percentage basis is defined by $VaR^{\%}_{\alpha} = z_{\alpha}\sigma$. $VaR^{\%}_{95\%} = (-1.645)\sigma$ and $VaR^{\%}_{99\%} = (-2.33)\sigma$ denote its 95% and 99% levels.

pandemic and economy (Cukierman 2011). In the next section, we proceed to algorithmic processing of COVID-19 and financial data based on operational research techniques.

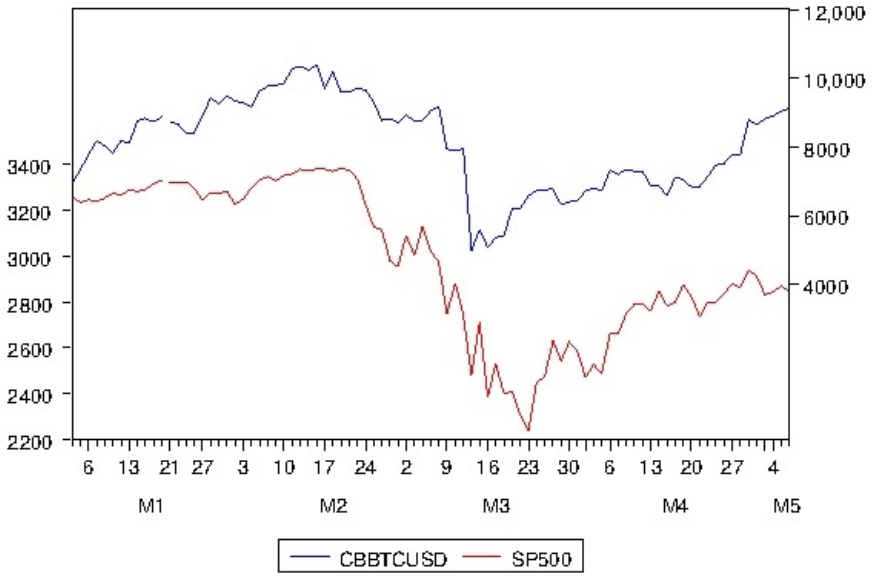

Figure 7. Price path of S&P 500 (left Y-axis) contrasted to that of Coinbase Bitcoin Price (right Y-axis) during the year 2020 in US $. Note: The data are sourced from St-Louis Federal Reserve Board (FRED). The Estimation period is 1 January 2020 to 6 May 2020. SP500 is the S&P 500, Index, Daily, Not Seasonally Adjusted. CBBTCUSD is the Coinbase Bitcoin, U.S. Dollars, Daily, Not Seasonally Adjusted. Both series are collected with a daily frequency.

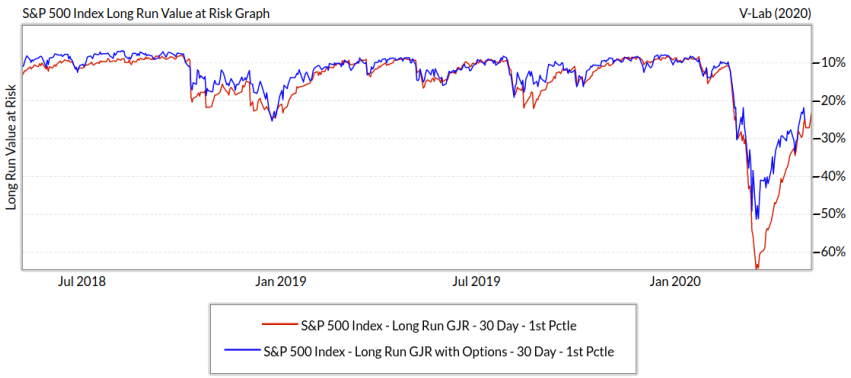

Figure 8. Value-at-Risk for S&P 500 computed either drom daily returns (in red) or from option prices (in blue). Note: the graph is produced by NYU Volatility Lab. The Estimation period is 8 May 2018 to 5 May 2020.

4. Linking the Disease to Predicted Economic Downturn

Data science comes in handy when in need for analyzing large chunks of data, as is the case with the depth of the epidemiological and clinical cases on COVID-19 on the one hand, and the heavy burden put on the servers by high-frequency financial data on the other hand.

We extract three main time-series for the world from the Johns Hopkins Coronavirus Center repository:

1. "ts-confirmed": time data of confirmed cases,
2. "ts-deaths": time series data of fatal cases, and
3. "ts-recovered": time series data of recovered cases.

These series have been thoroughly sourced by Section 2, and further documented in the Appendix A. We wish to reconstitute the series of events that stemmed from the COVID-19 outbreak to contagious effects on worldwide stock markets.

For this purpose, we encompass the closing returns from 31 stock markets based on the Oxford 'Realized Library' with an intra-daily frequency that reaches millions of transactions (2,587,175 at the time of accessing it). Tick-by-tick data are sampled over the five-minute horizon in order to avoid microstructure noise (see Barndorff-Nielsen et al. (2008) for the theory). Table 4 details the list of assets.

As a preliminary step, both databases of COVID-19 epidemiological cases and high-frequency financial data are merged by the time index.

4.1. Hierarchical Decision Tree for Visualizing the Influence of "ts-Confirmed" on Worldwide Stock Markets

In this section, we mobilize a tree algorithm with forward pruning (Breiman et al. 1984; Quinlan 1986; Smith and Nau 1994) in order to connect the epidemiological cases of COVID-19 (Section 2) to the downward market trends that were observed on stock markets (Section 3).

To feed the decision tree algorithm with stationary data, (i) COVID-19 cases are transformed to first-differences; and, (ii) stock markets data are transformed to log-returns.[10] This pre-processing step will allow for efficient splitting criteria.

The tree algorithm splits the merged data into nodes by class purity, with "COVID-19 cases" as the source and "Stock markets" returns as targets. Formally, let us write an adaptive basis-function model:

$$f(\mathbf{x}) = \mathbb{E}[y|\mathbf{x}] = \sum_{m=1}^{M} w_m \mathbb{I}(\mathbf{x} \in R_m) = \sum_{m=1}^{M} w_m \phi(\mathbf{x}; \mathbf{v}_m) \tag{5}$$

where R_m is the m'th region and w_m is the mean response in this region. $\mathbf{v}_m$ encodes the choice of variable to split on, and the threshold value, on the path from the root to the m'th leaf. The basis functions define the regions, and the weights specify the response values in each region (see Breiman et al. (1984); Quinlan (1986) for an introduction).

Use the following split function to find the optimal partitioning of the data:

$$(j^*, t^*) = \arg \min_{j \in \{1,\ldots,D\}} \min_{t \in \mathcal{T}_j} \text{cost}(\{\mathbf{x_i}, y_i : x_{ij} \leq t\}) + \text{cost}(\{\mathbf{x}_i, y_i : x_{ij} > t\}) \tag{6}$$

with $\mathcal{T}_j$ the set of possible thresholds for feature j by sorting the unique values of x_{ij} to a numeric value t. The most common approach is to consider splits $x_{ij} = c_k$ or $x_{ij} \neq c_k$ for each class label c_k.

When growing a decision tree, we can prevent over-fitting if the extra complexity of adding an extra sub-tree is not justified. The standard approach is to grow a "full" tree, and then to perform pruning. This methodological approach prevents data fragmentation, i.e., too little data fall into each sub-tree.

In order to determine how far to prune back, the scheme is to evaluate the branches on each sub-tree and pick the tree that gives the least increase in the chosen statistical error. To measure the quality of a split, we can resort to:

(i) a multinoulli model $\hat{\pi}_c = \frac{1}{|\mathcal{D}|} \sum_{i \in \mathcal{D}} \mathbb{I}(y_i = c)$ with $\mathcal{D}$ the data in the leaf by estimating class-conditional probabilities,

(ii) a misclassification rate by defining the most probable class label $\hat{y}_c = \arg\max_c \hat{\pi}_c$ and the corresponding error rate $\frac{1}{|\mathcal{D}|} \sum_{i \in \mathcal{D}} \mathbb{I}(y_i \neq \hat{y}) = 1 - \hat{\pi}_{\hat{y}}$,

[10] We can transmit unit root tests to interested readers to ensure that the series is $I(1)$ as such.

(iii) minimizing the entropy between the test leaf data and class label $\mathbb{H}(\hat{\mathfrak{K}}) = -\sum_{c=1}^{C} \hat{\pi}_c \log \hat{\pi}_c$, (or maximizing the information gain, see, e.g., Quinlan (1987)), or

(iv) a Gini index $\sum_{c=1}^{C} \hat{\pi}_c(1-\hat{\pi}_c) = \sum_c \hat{\pi}_c - \sum_c \hat{\pi}_c^2 = 1 - \sum_c \hat{\pi}_c^2$, with $\hat{\pi}_c$ the probability of a random entry in the leaf belongs to the class c, and $(1-\hat{\pi}_c)$ the probability of mis-classification.

In this paper, we favor cross-entropy and Gini measures.

Table 4. Oxford-Man's Realized Library: Database Statistics.

Symbol	Name	Earliest Available	Latest Available
.AEX	AEX index	3 January 2000	8 May 2020
.AORD	All Ordinaries	4 January 2000	8 May 2020
.BFX	Bell 20 Index	3 January 2000	8 May 2020
.BSESN	S&P BSE Sensex	3 January 2000	8 May 2020
.BVLG	PSI All-Share Index	15 October 2012	8 May 2020
.BVSP	BVSP BOVESPA Index	3 January 2000	8 May 2020
.DJI	Dow Jones Industrial Average	3 January 2000	8 May 2020
.FCHI	CAC 40	3 January 2000	8 May 2020
.FTMIB	FTSE MIB	1 June 2009	8 May 2020
.FTSE	FTSE 100	4 January 2000	7 May 2020
.GDAXI	DAX	3 January 2000	8 May 2020
.GSPTSE	S&P/TSX Composite index	2 May 2002	8 May 2020
.HSI	HANG SENG Index	3 January 2000	8 May 2020
.IBEX	IBEX 35 Index	3 January 2000	8 May 2020
.IXIC	Nasdaq 100	3 January 2000	8 May 2020
.KS11	Korea Composite Stock Price Index (KOSPI)	4 January 2000	8 May 2020
.KSE	Karachi SE 100 Index	3 January 2000	8 May 2020
.MXX	IPC Mexico	3 January 2000	8 May 2020
.N225	Nikkei 225	2 February 2000	8 May 2020
.NSEI	NIFTY 50	3 January 2000	8 May 2020
.OMXC20	OMX Copenhagen 20 Index	3 October 2005	7 May 2020
.OMXHPI	OMX Helsinki All Share Index	3 October 2005	8 May 2020
.OMXSPI	OMX Stockholm All Share Index	3 October 2005	8 May 2020
.OSEAX	Oslo Exchange All-share Index	3 September 2001	8 May 2020
.RUT	Russel 2000	3 January 2000	8 May 2020
.SMSI	Madrid General Index	4 July 2005	8 May 2020
.SPX	S&P 500 Index	3 January 2000	8 May 2020
.SSEC	Shanghai Composite Index	4 January 2000	8 May 2020
.SSMI	Swiss Stock Market Index	4 January 2000	8 May 2020
.STI	Straits Times Index	3 January 2000	8 May 2020
.STOXX50E	EURO STOXX 50	3 January 2000	8 May 2020

Figure 9 shows the result of the COVID-19 pandemic, as measured by the confirmed cases worldwide, on stock markets' panic during 2020-01-22 to 2020-05-05 (when last accessed the JHU repository at the time of writing the paper). Figure 9 shows the connection between financial markets. At the top of the tree is the financial market from which the contagion stems at the beginning of the health crisis. At the bottom of the tree, we find spillovers from the original contagion effect.

The resulting tree and decision boundaries are quite complex, even with prunning. The "top" stock market from which the COVID-19 pandemic spread is detected to be the French CAC 40 index

due to the hierarchical nature of the tree-growing process (FCHI, perhaps due to the announcement of the French president to lock-down the country on 16 March 2020).

Besides, we identify two main "paths" from which the pandemic spread to other financial markets:

1. On the left-hand side, we have the Australian All Ordinaries index (AORD). From Australia, financial contagion is then visible on sub-trees navigating through US small caps know as Russel 2000 (RUT), the Korean Kospi index (JS11), the UK FTSE, and then at the bottom of the tree reaching India's NIFTY 50 (NSEI), Pakistan's Stock Exchange (KSE), the US Standard & Poor's 500 (SPX) or the Japanese NIKKEI (N225). Stemming from the overarching "top" of France and first "branch" Australia, we notice as well other sub-trees channeling though the US Dow Jones Industrial Average (DJI) with more pronounced regional effects on Canada's (GSPTSE) and Mexico's (MXX) stock exchanges until we reach the bottom of the tree.
2. On the right-hand side, we identify the EURO STOXX 50 (STOXX50E). Contagion occurs immediately on the first sub-tree on the Amsterdam stock exchange (AEX) with spillovers in Switzerland (SSMI), Sweden (OMXSPI), and Norway (OSEAX), until Denmark (OMXC20) at the bottom of the tree. On the second sub-tree (far right of Figure 9), we visualize that the financial crisis ultimately reaches other European countries, such as Spain (IBEX), Belgium (BFX), and Finland (OMXHPI). Inter-regional spillovers to Brazil (BVSP, through Spain) and Singapore (STI, through EURO STOXX) are also visible at the bottom of the tree.

This first strand of the result suggests that contagion first occurred on European and Australasian stock markets, as the number of COVID-19 confirmed cases was precisely documented and raised swift public policy responses. If, instead, we plug in the time series "ts-deaths" or "ts-recovered", we verify that the decision tree that is reproduced in Figure 9 is stable, i.e., small changes to the input data (of the same information content) do not have substantial effects on the structure of the tree.[11]

4.2. Experimenting Mosaic Plots with the Series "ts-Death" on 2020-03-16

Next, in Figure 10 we inspect a Mosaic plot for the day 2020-03-16 that seemed so important as to place France at the top of the hierarchical tree. Recall that the French president implemented a 45-day lock-down of the country on that date, which seems from our preliminary data analysis to have wreaked havoc on financial markets.

Mosaic graphs allow visualizing data across two or more dimensions. They are handy when attempting to capture the relationships between different variables, as in our setting. The Mosaic plot's statistical analysis as a contingency table is covered by Friendly (2002).

In Figure 10, the dimensions we are plotting are the following:

- bottom: date chosen for the Mosaic is specifically 2020-03-16;
- left: closing daily prices for stock markets;
- top: intra-day transactions on stock markets; and,
- right: number of deaths reported worldwide on that day according to JHU/CCSE repository.

[11] For the sake of brevity, corresponding trees for "ts-deaths" and "ts-recovered" has been saved to disk and can be sent upon request.

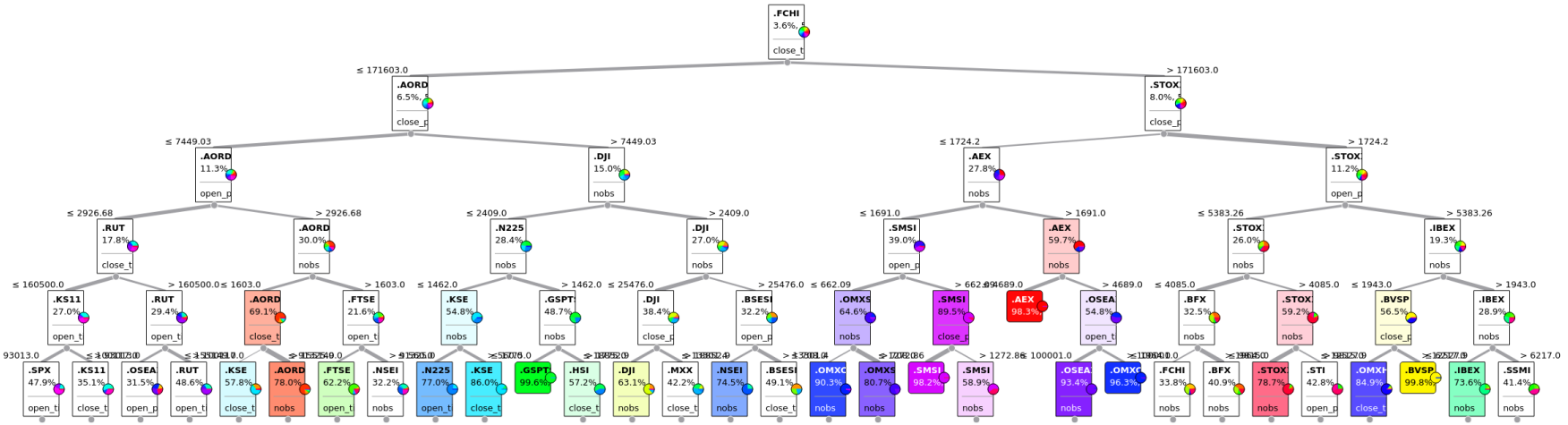

Figure 9. Tree for Origin "ts-confirmed" and Target "Stock markets". Note: The origin of the tree is COVID-19 confirmed cases worldwide. The Estimation period is 22 January 2020 to 5 May 2020. The first column of Table 4 provides tickers for Stock markets.

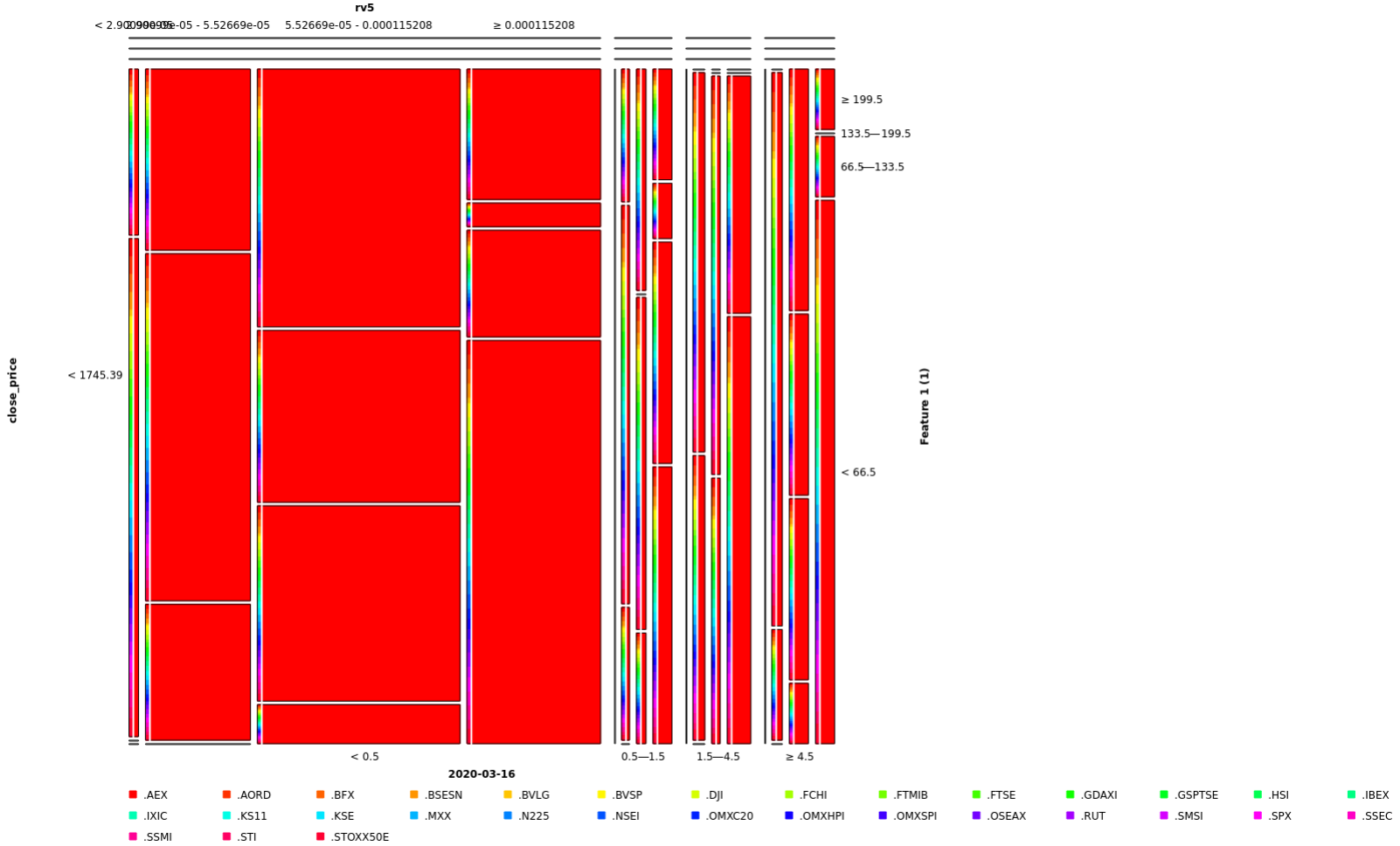

Figure 10. Mosaic plot on 2020-03-16 for series "ts-death" and "Stock markets".

The end result unequivocally paints a "red" picture of how the pandemic, and the incredibly worrying trend in deaths worldwide, has spread to financial markets, with some of them even briefly suspending trading (such as the NYSE) during these troubling events. This picture illustrates perfectly, that, in our opinion, for money managers in such a contagious financial environment with spillovers of downward closing prices on each stock market, there is "no place to hide". Had we found other colors predominant on the Mosaic (e.g., shades of blue or green), we could have advised moving the funds safely here or there, but there is not such a place (other candidates "safe-havens", such as Gold or even Bitcoin, have been discussed in Section 3).

To grasp the meaning of Figure 10 visually, the reader can view it as a carpet plot linking returns on financial markets. Usually, when such a plot is posted on Twitter about Wall Street blue chips, it shows the extent to how a piece of news (say, the Boeing 737 MAX industrial disaster) has expanded into stock markets. They are usually in a net winners or net losers situation. Against the COVID-19 pandemic, what Figure 10 shows, is that there are only losers on financial markets in such circumstances, highlighting the fact mentioned in the previous Section that there is no place to hide for asset managers to build alpha strategies.

4.3. A Final Look at the Pythagorean Forest of Influence of "ts-Recovered" on Stock Markets

If we seek to end this paper on a more positive outlook, then we might move the decision tree upside-down and present it as a forest. To that end, we employ the series "ts-recovered", which should be a reason for "rebirth" for the economy, as some patients naturally heal from the COVID-19 (in the absence of effective treatment at the time of writing, waiting for clinical experiments from Pfizer and Moderna vaccines).

In Figure 11, we reproduce a Pythagorean Forest, which visualizes how from the tree trunk of "ts-recovered" new branches and leaves can grow back on financial markets. The Pythagorean Forest stems from a decision tree model, called "random forest", where each visualization pertains to one randomly constructed tree. Its construction is covered by Beck et al. (2014).

Without loss of generality, consider Pythagorean Trees (H_v, S) :, where $H_v = (V, E)$ is a binary hierarchy of $V = \{v_1, \ldots, v_k\}$ set of k vertices and $E \subset V \times V$ finite set of edges. $S = (c, \Delta s, \theta)$ is the initial square with center c, length of the sides Δs, and slope angle θ. The recursive procedure first draws square S and proceeds if the current hierarchy still contains more than a single node. Subsequently, encoding the node weights in the squares' size, the angles α and β are computed according to the normalized weight of the node opposed to the angle. The width Δx_i of a rectangle R_i can be changed by modifying the corresponding angle α_i accordingly. It should reflect weight $w_x(v_i)$ of a vertex v_i in relation to the weight of its siblings:

$$\alpha_i := \pi \times \frac{w_x(v_i)}{\sum_{j=1}^{n} w_x(v_j)} \tag{7}$$

The width of the rectangle is $\Delta x_i := \Delta x \times \sin \frac{\alpha_j}{2}$, where Δx is the width of the parent node. A maximum branching factor can be implemented. The human reader automatically connects the rectangles on the curve, which is denoted as the law of continuation.

Figure 11 represents another kind of tree: a "forest", so to speak since we are concerned here with patients that recovered from the COVID-19. The goal is to show by a myriad of colors how the increased number of healing is being transmitted to the various stock markets in the database under increased market gains. Although being complex to construct, such fractal images exhibit aesthetic properties, which makes these images easier to interpret. The Pythagorean Forest emphasizes the influence of the root—which is "ts-recovered"—and its hierarchical influence on subsets down to the level of unitary stock markets. The root node fills the graph with white color. Its immediate descendants can be understood as higher-level nodes of the forest.

The image shows that, among the leading directories, the most meaningful parent-child relationships are to be found with the EURO STOXX 50 (Stoxx50E) in red color; the Amsterdam (AEX), Brussels (BFX), and Australian (AORD) stock markets in orange color; the French CAC 40 (FCHI) and Dow Jones Industrial Average (DJI) in light green color; and, the Nordic stock markets of Copenhagen, Helsinki, and Stockholm (OMXC20, OMXHPI, OMXSPI) in purple colors. This finding confirms the decision tree based on "ts-confirmed", where we dated back the origins of the financial contagion to European and Australasian market, and the U.S. as a repercussion of lock-down implemented in these countries beforehand.

If we move away from the most prominent nodes to the forest's secondary level, then we can notice other sub-vertices, each displaying their own set of edges. The granularity of the results obtained with this visualization tool is remarkable without zooming too much into detail. It is perceptible how the world economy can "heal" from the Coronavirus as more patients recover from it down to the level of individual stock markets. For instance, on the forest's right-hand side, we can see the effects of recovering Amsterdam or Brussels stock exchanges on the Milan or Frankfurt market places (FTMIB and GDAXI, respectively, in light green)—hence, these nodes are connected in the sub-hierarchy of the forest.

Overall, we gained an overview of the main branches connecting the COVID-19 epidemiological cases to the world stock markets. This result's beauty is that we achieved it without restricting, *a-priori*, the number of vertices (e.g., arbitrary hierarchies are allowed).

To further explain our results intuitively, we point out that asset markets are susceptible to the news. Whenever pharmaceutical companies, like Pfizer, or start-ups, like Moderna, announce 95% of positive results on their COVID-19 vaccines, the financial markets react very positively with day-to-day increased returns. In our sample, the intuition is that COVID-19 cases are quickly developing worldwide, which incites stock markets to decline and be linked altogether into a recession circle. However, the extra data-science experiment illustrates that the global economy can be seen as a tree whose leaf can become green again (as patients heal, or the vaccine will be mass-administered). Therefore, financial contagion would bring a new virtuous circle of prosperous economic growth in the globalized economy.

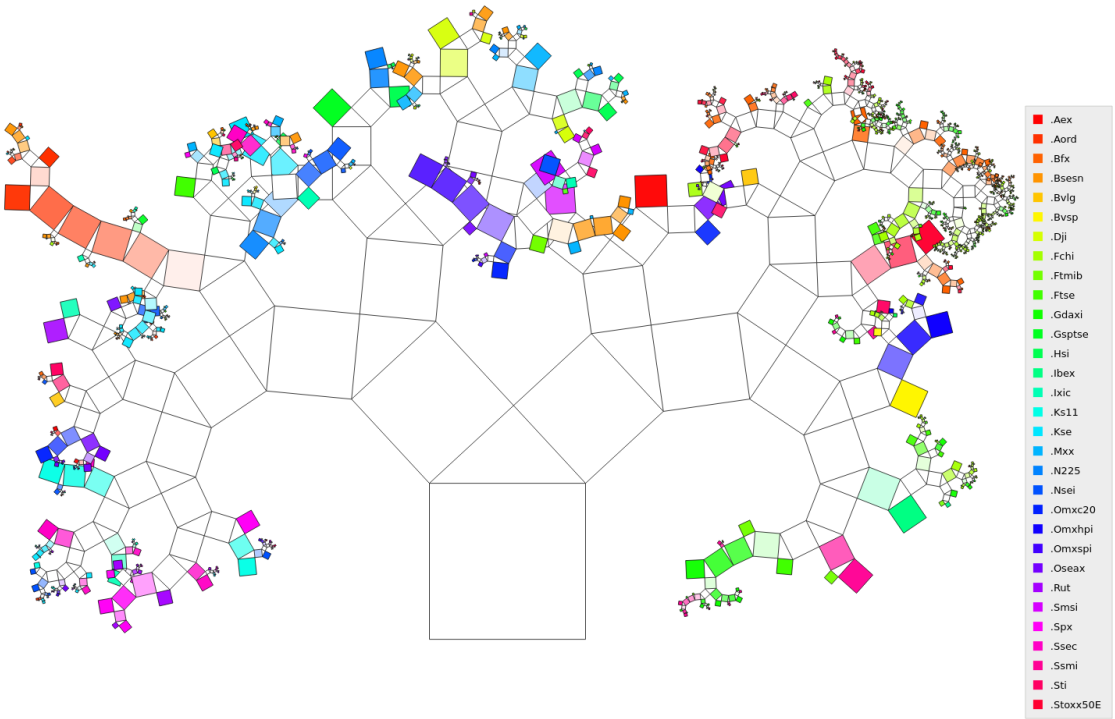

Figure 11. Pythagorean forest for series "ts-recovered" and "Stock markets". Note: the origin of the forest is COVID-19 recovered cases worldwide. The estimation period is 22 January to 5 May 2020. Tickers for Stock markets are given in the first column of Table 4.

5. Concluding Remarks

As a proteiform disease, COVID-19 is drowning the macro-financial environment into a recession that it is too early to foreshadow. All in all, confronting several stakeholders' views amid the COVID-19 outbreak has brought this research a myriad of facts. By merging health and stock market databases, three types of robust scientific methods have been mobilized in this paper:

1. epidemiological;
2. financial from quants' viewpoint; and,
3. algorithmic from a data scientist's viewpoint.

The original contribution is to document the effects of the COVID-19 pandemic on financial contagion. For the wide dissemination of research results, this paper has opted for a low-key approach on the technicalities that underlie the models estimated as a methodological choice of the authors.

Whereas decision trees and mosaic plots revealed a heavy concentration of stock markets plummeting on 16 March 2020 (following a peak of infection detected on 3 March), brighter perspectives of re-birth: of the economy have been envisioned based on a Pythagorean forest that illustrates the positive effects of more patients "healing" from the disease.

Given the level of integration of the global financial system, the eminent risk of financial contagion may further accentuate the global systemic risk. While economies currently at different growth paths are faced with unique macroeconomic conditions that determine the stability and resilience of their respective financial systems, the different policy responses that are adopted by different economies in combating the pandemic will, to a large extent, determine the severity, duration, and management of both the health and consequent crisis with spillover effects expected (Battiston et al. 2012).

In this regard, while the policy response in one country may help to shield the economy from domestic adverse economic effects, cross-border financial system interactions may enhance global financial distress, as vulnerability from one economy is transmitted to other financial systems. Ultimately, interdependence and the presence of financial contagion mean that the financial system is as stable as its weakest link.

Therefore, global economies' ability to effectively manage the impending crisis will depend on: (i) the effectiveness of individual policy response and (ii) the global financial systems' ability to effectively absorb negative spillovers and adverse economic shocks. Systemic risk management will play a key role in enhancing financial systems' resilience and providing much-needed financial intermediation services to the economy. In this regard, continuous analysis and monitoring of the financial system's ability remain paramount to realize overall macroeconomic stability (Gunay 2020a).

The study implications relate to the cataclysmic impact of the COVID-19 pandemic on financial markets. The recession is expected to be severe. Financial contagion is in motion, not only across asset markets, but also across countries. The "silver bullet" to get out of the danger zone would be the swift deployment of vaccines in the years 2021–22 in order to achieve community resistance to COVID-19.

Regarding future research in this area of banking and finance, the type of data that are needed to analyze systemic risk and contagion would include (i) individual banks balance sheet and financial ratios, (ii) cross-sector loans and bonds from financial institutions to the real economy sector, and (iii) cross border loans and bonds.

The study limitations are based on the restricted data sample at the beginning of the pandemic. Several years of observations on the consequences of the COVID-19 on global economies will help to put this first set of results into perspective as data gathering evolves in the scientific community.

Funding: This research received no external funding.

Conflicts of Interest: The author declares no conflict of interest.

Appendix A

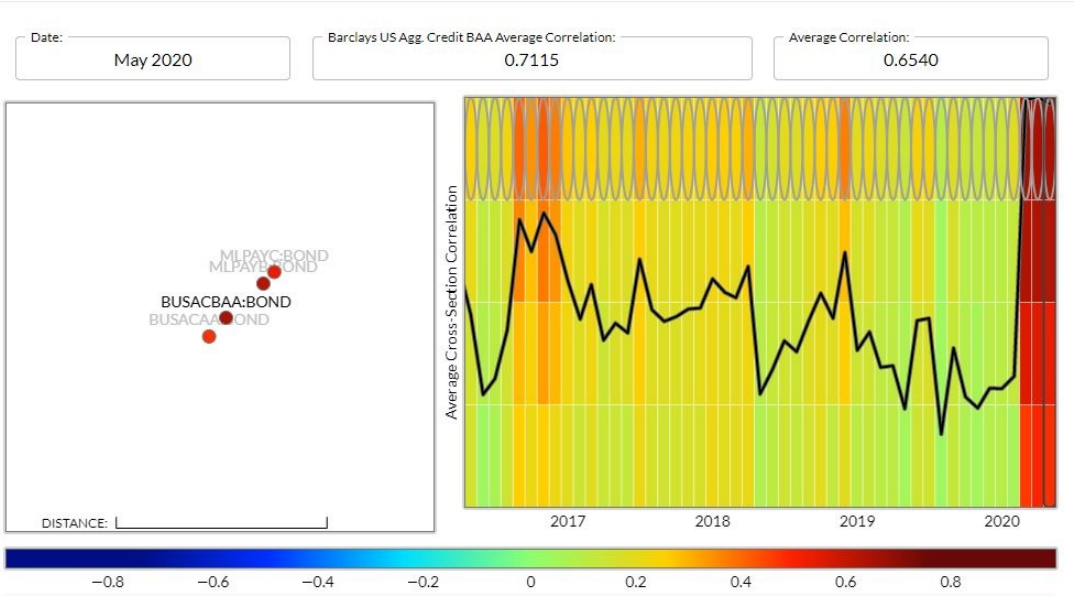

Figure A1. Correlation Analysis for Bonds as extracted from DCC(1,1). Note: The graph is produced by NYU Volatility Lab. The Estimation period is 6 May 1996 to 1 May 2020. The Bonds dataset contains the following series: Bank of America ML HY Cash Pay B All (MLPAYB) Bank of America ML HY Cash Pay C All (MLPAYC) Barclays US Agg. Credit AA (BUSACAA) Barclays US Agg. Credit BAA (BUSACBAA).

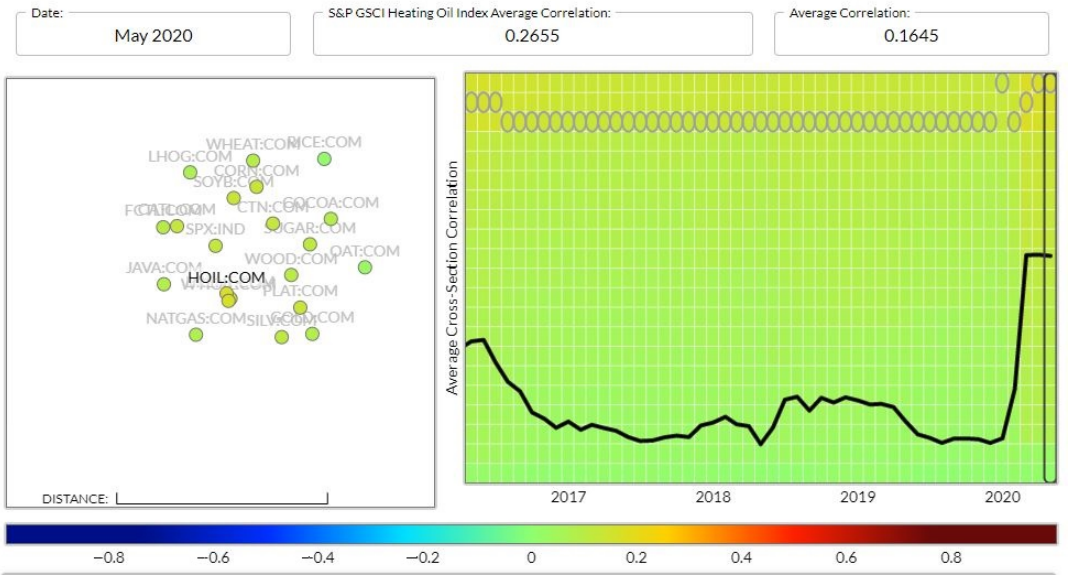

Figure A2. Correlation Analysis for Commodities as extracted from DCC(1,1). Note: The graph is produced by NYU Volatility Lab. The Estimation period is 17 January 2002 to 1 May 2020. The Commodities dataset contains the following series: CBT-Rough Rice Composite Futures Continuous (RICE) Gold Spot (GOLD) Lumber, Generic 1st (WOOD) Oats, Generic 1st (OAT) S&P 500 Index (SPX) S&P GSCI Brent Crude Oil Index (BRENT) S&P GSCI Cocoa Index (COCOA) S&P GSCI Coffee Index (JAVA) S&P GSCI Corn Index (CORN) S&P GSCI Cotton Index (CTN) S&P GSCI Feeder Cattle Index (FCTL) S&P GSCI Heating Oil Index (HOIL) S&P GSCI Lean Hogs Index (LHOG) S&P GSCI Live Cattle Index (CATL) S&P GSCI Natural Gas Index (NATGAS) S&P GSCI Platinum Index (PLAT) S&P GSCI Soybeans Index (SOYB) S&P GSCI Sugar Index (SUGAR) S&P GSCI Wheat Index (WHEAT) S&P GSCI WTI Crude Oil Index (WTIOIL) Silver Spot (SILV).

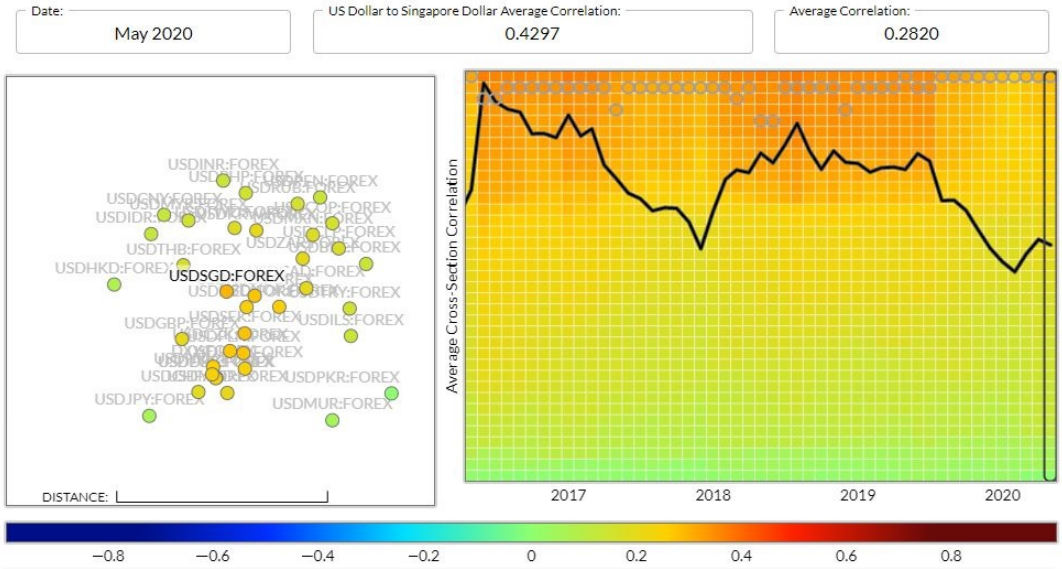

Figure A3. Correlation Analysis for Exchange Rates as extracted from DCC(1,1). Note: The graph is produced by NYU Volatility Lab. The Estimation period is 3 August 2000 to 1 May 2020. The Exchange Rates dataset contains the following series: United States Dollar Index (DXY) US Dollar to Australian Dollar (AUD) US Dollar to Brazilian Real (BRL) US Dollar to British Pound (GBP) US Dollar to Canadian Dollar (CAD) US Dollar to Chilean Peso (CLP) US Dollar to Chinese Renminbi (CNY) US Dollar to Colombian Peso (COP) US Dollar to Croatian Kuna (HRK) US Dollar to Czech Koruna (CZK) US Dollar to Danish Krone (DKK) US Dollar to Euro (EUR) US Dollar to Hong Kong Dollar (HKD) US Dollar to Hungarian Forint (HUF) US Dollar to Indian Rupee (INR) US Dollar to Indonesian Rupiah (IDR) US Dollar to Israeli Shekel (ILS) US Dollar to Japanese Yen (JPY) US Dollar to Malaysian Ringgit (MYR) US Dollar to Mauritian Rupee (MUR) US Dollar to Mexican Peso (MXN) US Dollar to Moroccan Dirham (MAD) US Dollar to New Zealand Dollar (NZD) US Dollar to Norwegian Krone (NOK) US Dollar to Pakistani Rupee (PKR) US Dollar to Peruvian New Sol (PEN) US Dollar to Philippine Peso (PHP) US Dollar to Polish Zloty (PLN) US Dollar to Russian Ruble (RUB) US Dollar to Singapore Dollar (SGD) US Dollar to South African Rand (ZAR) US Dollar to South Korean Won (KRW) US Dollar to Swedish Krona (SEK) US Dollar to Swiss Franc (CHF) US Dollar to Taiwanese Dollar (TWD) US Dollar to Thai Baht (THB) US Dollar to Turkish New Lira (TRY).

Table A1. Aggregated Data Ordered By Confirmed Cases available from JHU/CCSE repository on 2020-05-05.

	Location	Confirmed	Perc. Confirmed	Deaths	Perc. Deaths	Recovered	Perc. Recovered	Active	Perc. Active
1	Spain	219,329	5.99	25,613	11.68	123,486	56.30	70,230	32.02
2	Italy	213,013	5.82	29,315	13.76	85,231	40.01	98,467	46.23
3	United Kingdom	194,990	5.32	29,427	15.09	0	0.00	165,563	84.91
4	NYC, NY, USA	176,874	4.83	19,067	10.78	0	0.00	157,807	89.22
5	France	168,935	4.61	25,498	15.09	51,803	30.66	91,634	54.24
6	Germany	167,007	4.56	6993	4.19	135,100	80.89	24,914	14.92
7	Russia	155,370	4.24	1451	0.93	19,865	12.79	134,054	86.28
8	Turkey	129,491	3.54	3520	2.72	73,285	56.59	52,686	40.69
9	Brazil	115,455	3.15	7938	6.88	48,221	41.77	59,296	51.36
10	Iran	99,970	2.73	6340	6.34	80,475	80.50	13,155	13.16

Number of Countries/Regions reported: 187; Number of Cities/Provinces reported: 138; Unique number of distinct geographical locations combined: 3209.

Table A2. Aggregated Data Ordered By Deaths available from JHU/CCSE repository on 2020-05-05.

	Location	Confirmed	Perc. Confirmed	Deaths	Perc. Deaths	Recovered	Perc. Recovered	Active	Perc. Active
1	United Kingdom	194,990	5.32	29,427	15.09	0	0.00	165,563	84.91
2	Italy	213,013	5.82	29,315	13.76	85,231	40.01	98,467	46.23
3	Spain	219,329	5.99	25,613	11.68	123,486	56.30	70,230	32.02
4	France	168,935	4.61	25,498	15.09	51,803	30.66	91,634	54.24
5	NYC, NY, USA	176,874	4.83	19,067	10.78	0	0.00	157,807	89.22
6	Belgium	50,509	1.38	8016	15.87	12,441	24.63	30,052	59.50
7	Brazil	115,455	3.15	7938	6.88	48,221	41.77	59,296	51.36
8	Germany	167,007	4.56	6993	4.19	135,100	80.89	24,914	14.92
9	Iran	99,970	2.73	6340	6.34	80,475	80.50	13,155	13.16
10	Netherlands	41,087	1.12	5168	12.58	0	0.00	35,919	87.42

Number of Countries/Regions reported: 187; Number of Cities/Provinces reported: 138; Unique number of distinct geographical locations combined: 3209.

Table A3. Aggregated Data Ordered By Recovered Cases available from JHU/CCSE repository on 2020-05-05.

	Location	Confirmed	Perc. Confirmed	Deaths	Perc. Deaths	Recovered	Perc. Recovered	Active	Perc. Active
1	Recovered, US	0	0.00	0	NaN	189,791	NaN	−160,761	NaN
2	Germany	167,007	4.56	6993	4.19	135,100	80.89	24,914	14.92
3	Spain	219,329	5.99	25,613	11.68	123,486	56.30	70,230	32.02
4	Italy	213,013	5.82	29,315	13.76	85,231	40.01	98,467	46.23
5	Iran	99,970	2.73	6340	6.34	80,475	80.50	13,155	13.16
6	Turkey	129,491	3.54	3520	2.72	73,285	56.59	52,686	40.69
7	China.Hubei	68,128	1.86	4512	6.62	63,616	93.38	0	0.00
8	France	168,935	4.61	25,498	15.09	51,803	30.66	91,634	54.24
9	Brazil	115,455	3.15	7938	6.88	48,221	41.77	59,296	51.36
10	Recovered, Canada	0	0.00	0	NaN	27,006	NaN	−27,006	NaN

Number of Countries/Regions reported: 187; Number of Cities/Provinces reported: 138; Unique number of distinct geographical locations combined: 3209.

Table A4. Aggregated Data Ordered By Active Cases available from JHU/CCSE repository on 2020-05-05.

	Location	Confirmed	Perc. Confirmed	Deaths	Perc. Deaths	Recovered	Perc. Recovered	Active	Perc. Active
1	United Kingdom	194,990	5.32	29,427	15.09	0	0.00	165,563	84.91
2	NYC, NY, USA	176,874	4.83	19,067	10.78	0	0.00	157,807	89.22
3	Russia	155,370	4.24	1451	0.93	19,865	12.79	134,054	86.28
4	Italy	213,013	5.82	29,315	13.76	85,231	40.01	98,467	46.23
5	France	168,935	4.61	25,498	15.09	51,803	30.66	91,634	54.24
6	Spain	219,329	5.99	25,613	11.68	123,486	56.30	70,230	32.02
7	Brazil	115,455	3.15	7938	6.88	48,221	41.77	59,296	51.36
8	Turkey	129,491	3.54	3520	2.72	73,285	56.59	52,686	40.69
9	Cook, Illinois, USA	45,223	1.23	1922	4.25	0	0.00	43,301	95.75
10	Netherlands	41,087	1.12	5168	12.58	0	0.00	35,919	87.42

Number of Countries/Regions reported: 187; Number of Cities/Provinces reported: 138; Unique number of distinct geographical locations combined: 3209.

Table A5. Top-ten Contributors to the Time Series of Confirmed Cases available from JHU/CCSE repository on 2020-05-05.

	Worldwide	**ts-Confirmed**	**Totals:**	**3,662,691**					
Country. Region	**Province. State**	**Totals**	**GlobalPerc**	**LastDayChange**	$t-2$	$t-3$	$t-7$	$t-14$	$t-30$
1	US	1,204,351	32.88	23,976	22,335	25,501	27,327	28,486	29,515
2	Spain	219,329	5.99	1318	545	884	2144	4211	5029
3	Italy	213,013	5.82	1075	1221	1389	2086	3370	3599
4	United Kingdom	194,990	5.32	4406	3985	4339	4076	4451	3802
5	France	168,935	4.61	1049	614	296	−2512	−2206	3912
6	Germany	167,007	4.56	855	488	697	1627	2357	3251
7	Russia	155,370	4.24	10,102	10,581	10,633	5841	5236	954
8	Turkey	129,491	3.54	1832	1614	1670	2936	3083	3148
9	Brazil	115,455	3.15	6835	6794	4726	6450	2678	1031
10	Iran	99,970	2.73	1323	1223	976	1073	1194	2274

Global Perc, Average: 0.38 (sd: 2.17)
Global Perc. Average in top 10: 7.28 (sd: 9.06)

Number of Countries/Regions reported: 187; Number of Cities/Provinces reported: 83; Unique number of distinct geographical locations combined: 266.

Table A6. Top-ten Contributors to the Time Series of Deaths available from JHU/CCSE repository on 2020-05-05.

	Worldwide	**ts-Deaths**	**Totals:**	**257,239**					
Country. Region	**Province. State**	**Totals**	**GlobalPerc**	**LastDayChange**	$t-2$	$t-3$	$t-7$	$t-14$	$t-30$
1	US	71,064	5.90	2142	1240	1313	2612	2326	1519
2	United Kingdom	29,427	15.09	693	288	315	795	837	568
3	Italy	29,315	13.76	236	195	174	323	437	636
4	Spain	25,613	11.68	185	164	164	453	435	700
5	France	25,498	15.09	330	304	135	427	544	833
6	Belgium	8016	15.87	92	80	79	170	264	185
7	Brazil	7938	6.88	571	316	290	430	165	78
8	Germany	6993	4.19	0	127	54	153	246	226
9	Iran	6340	6.34	63	74	47	80	94	136
10	The Netherlands	5168	12.58	86	26	69	145	138	101

Number of Countries/Regions reported: 187; Number of Cities/Provinces reported: 83; Unique number of distinct geographical locations combined: 266.

Table A7. Top-ten Contributors to The time Series of Recovered Cases available from JHU/CCSE repository on 2020-05-05.

	Worldwide	ts-Recovered	Totals:	1,198,832				
Country. Region	**Province. State**	**Totals**	**LastDayChange**	$t-2$	$t-3$	$t-7$	$t-14$	$t-30$
1	US	189,791	2611	7028	4770	4784	2162	2133
2	Germany	135,100	2400	2100	1600	3000	4200	0
3	Spain	123,486	2143	2441	1654	6399	3401	2357
4	Italy	85,231	2352	1225	1740	2311	2943	1022
5	Iran	80,475	1096	957	1072	1352	2148	4500
6	Turkey	73,285	5119	5015	4892	5231	1559	284
7	China.Hubei	63,616	0	0	0	0	5	69
8	France	51,803	1365	465	222	1341	1445	1067
9	Brazil	48,221	2406	2824	2054	1588	2327	0
10	Canada	27,006	976	1109	1107	1096	1266	244

Number of Countries/Regions reported: 187; Number of Cities/Provinces reported: 68; Unique number of distinct geographical locations combined: 252.

References

Akhtaruzzaman, Md, Sabri Boubaker, and Ahmet Sensoy. 2020. Financial contagion during covid–19 crisis. *Finance Research Letters* 101604. [CrossRef]

Al-Awadhi, Abdullah M., Khaled Al-Saifi, Ahmad Al-Awadhi, and Salah Alhamadi. 2020. Death and contagious infectious diseases: Impact of the covid-19 virus on stock market returns. *Journal of Behavioral and Experimental Finance* 27: 100326. [CrossRef] [PubMed]

Andersen, Kristian G., Andrew Rambaut, W. Ian Lipkin, Edward C. Holmes, and Robert F. Garry. 2020. The proximal origin of sars-cov-2. *Nature Medicine* 26: 450–52. [CrossRef] [PubMed]

Ashraf, Badar Nadeem. 2020. Stock markets' reaction to covid-19: Cases or fatalities? *Research in International Business and Finance* 101249. [CrossRef]

Bae, Kee-Hong, G. Andrew Karolyi, and Reneé M. Stulz. 2003. A new approach to measuring financial contagion. *The Review of Financial Studies* 16: 717–63. [CrossRef]

Bailey, Norman. 1975. *The Mathematical Theory of Infectious Diseases*. London: Griffin.

Baker, Scott R., Nicholas Bloom, Steven J. Davis, Kyle Kost, Marco Sammon, and Tasaneeya Viratyosin. 2020. The unprecedented stock market reaction to covid-19. *The Review of Asset Pricing Studies* 10: 742–58. [CrossRef]

Barndorff-Nielsen, Ole E., Peter Reinhard Hansen, Asger Lunde, and Neil Shephard. 2008. Designing realized kernels to measure the ex post variation of equity prices in the presence of noise. *Econometrica* 76: 1481–536.

Battiston, Stefano, Domenico Delli Gatti, Mauro Gallegati, Bruce Greenwald, and Joseph E. Stiglitz. 2012. Liaisons dangereuses: Increasing connectivity, risk sharing, and systemic risk. *Journal of Economic Dynamics and Control* 36: 1121–41. [CrossRef]

Beck, Fabian, Michael Burch, Tanja Munz, Lorenzo Di Silvestro, and Daniel Weiskopf. 2014. Generalized pythagoras trees for visualizing hierarchies. Paper presented at 2014 International Conference on Information Visualization Theory and Applications (IVAPP), Lisbon, Portugal, January 5–8, pp. 17–28.

Bollerslev, Tim. 1986. Generalized autoregressive conditional heteroskedasticity. *Journal of Econometrics* 31: 307–27. [CrossRef]

Breiman, Leo, Jerome Friedman, Charles J Stone, and Richard A Olshen. 1984. *Classification and Regression Trees*. New York: CRC Press.

Buraschi, Andrea, Robert Kosowski, and Fabio Trojani. 2014. When there is no place to hide: Correlation risk and the cross-section of hedge fund returns. *The Review of Financial Studies* 27: 581–616. [CrossRef]

Cheema, Muhammad A., Robert W. Faff, and Kenneth Szulczuk. 2020. The 2008 global financial crisis and covid-19 pandemic: How safe are the safe haven assets? *Covid Economics, Vetted and Real-Time Papers* 34: 88–115. [CrossRef]

Clancy, Damian. 2014. Sir epidemic models with general infectious period distribution. *Statistics & Probability Letters* 85: 1–5.

Conlon, Thomas, and Richard McGee. 2020. Safe haven or risky hazard? bitcoin during the covid-19 bear market. *Finance Research Letters* 35: 101607. [CrossRef] [PubMed]

Corbet, Shaen, Charles Larkin, and Brian Lucey. 2020. The contagion effects of the covid-19 pandemic: Evidence from gold and cryptocurrencies. *Finance Research Letters* 35: 101554. [CrossRef]

Cukierman, Alex. 2011. Reflections on the crisis and on its lessons for regulatory reform and for central bank policies. *Journal of Financial Stability* 7: 26–37. [CrossRef]

Engle, Robert F., and Kevin Sheppard. 2001. *Theoretical and Empirical Properties of Dynamic Conditional Correlation Multivariate Garch*. Technical Report, Working Paper #8554. Cambridge: National Bureau of Economic Research.

Forbes, Kristin J., and Roberto Rigobon. 2002. No contagion, only interdependence: Measuring stock market comovements. *The Journal of Finance* 57: 2223–61. [CrossRef]

Friendly, Michael. 2002. A brief history of the mosaic display. *Journal of Computational and Graphical Statistics* 11: 89–107. [CrossRef]

Gunay, Samet. 2020a. COVID-19 pandemic versus global financial crisis: Evidence from currency market. *Working Paper SSRN* 3584249. Available online: https://ssrn.com/abstract=3584249 (accessed on 1 December 2020).

Gunay, Samet. 2020b. A new form of financial contagion: COVID-19 and stock market responses. *Working Paper SSRN* 3584243. Available online: http://dx.doi.org/10.2139/ssrn.3584243 (accessed on 1 December 2020).

Ji, Qiang, Dayong Zhang, and Yuqian Zhao. 2020. Searching for safe-haven assets during the covid-19 pandemic. *International Review of Financial Analysis* 71: 101526. [CrossRef]

Jorion, Philippe. 2000. *Value at Risk*. New York: The McGraw-Hill Companies.

Martínez-Jaramillo, Serafín, Omar Pérez Pérez, Fernando Avila Embriz, and Fabrizio López Gallo Dey. 2010. Systemic risk, financial contagion and financial fragility. *Journal of Economic Dynamics and Control* 34: 2358–74. [CrossRef]

Papadamou, Stephanos, Athanasios Fassas, Dimitris Kenourgios, and Dimitrios Dimitriou. 2020. *Direct and Indirect Effects of COVID-19 Pandemic on Implied Stock Market Volatility: Evidence from Panel Data Analysis*. MPRA Working Paper. Munich: Munich Personal RePEc Archive.

Quinlan, J. Ross. 1986. Induction of decision trees. *Machine Learning* 1: 81–106. [CrossRef]

Quinlan, J. Ross. 1987. Simplifying decision trees. *International Journal of Man-Machine Studies* 27: 221–34. [CrossRef]

Shamsi Naima, Ali Torabi, and Hemet Shakouri G. 2018. An option contract for vaccine procurement using the sir epidemic model. *European Journal of Operational Research* 267: 1122–40. [CrossRef]

Sharif, Arshian, Chaker Aloui, and Larisa Yarovaya. 2020a. COVID-19 pandemic, oil prices, stock market and policy uncertainty nexus in the us economy: Fresh evidence from the wavelet-based approach. *SSRN Working Paper* 3574699. Available online: https://papers.ssrn.com/sol3/papers.cfm?abstract_id=3574699 (accessed on 1 December 2020).

Sharif, Arshian, Chaker Aloui, and Larisa Yarovaya. 2020b. COVID-19 pandemic, oil prices, stock market, geopolitical risk and policy uncertainty nexus in the us economy: Fresh evidence from the wavelet-based approach. *International Review of Financial Analysis* 70: 101496. [CrossRef]

Smith, Stephen J. J., and Dana S. Nau. 1994. An analysis of forward pruning. Paper presented at the Association for the Advancement of Artificial Intelligence, Seattle, WA, USA, July 31–August 4, pp. 1386–91.

Taleb, Nassim Nicholas. 2007. *The Black Swan: The Impact of the Highly Improbable*. London: Random House Trade Paperbacks, vol. 2.

Zaremba, Adam, Renatas Kizys, David Y. Aharon, and Ender Demir. 2020. Infected markets: Novel coronavirus, government interventions, and stock return volatility around the globe. *Finance Research Letters* 35: 101597. [CrossRef] [PubMed]

Zhang, Dayong, Min Hu, and Qiang Ji. 2020. Financial markets under the global pandemic of covid-19. *Finance Research Letters* 36: 101528. [CrossRef] [PubMed]